Progress in numerical simulations of systems with a $\theta-$vacuum like term: The two and three-dimensional Ising model within an imaginary magnetic field

Vicente Azcoiti, Eduardo Follana and Alejandro Vaquero,

Departamento de Física Teórica, Facultad de Ciencias, Universidad de Zaragoza
C/ Pedro Cerbuna 12, E-50009, Zaragoza (Spain)

January 20, 2013

Abstract

Using the approach developed in [1], we succeeded in reconstructing the behaviour of the antiferromagnetic Ising model with imaginary magnetic field $i\theta$ for two and three dimensions in the low temperature regime. A mean-field calculation, expected to work well for high dimensions, is also carried out, and the mean-field results coincide qualitatively with those of the two- and three-dimensional Ising model. The mean field analysis reveals also a phase structure more complex than the one expected for QCD with a topological $\theta-$term.

1 Introduction

Quantum field theories with complex actions are systems as interesting as difficult to analyze: on one hand, the complex action usually gives rise to a severe sign problem, which prevents computer simulations to be performed; on the other hand, the number of known, exactly solvable models with complex actions is quite limited. And yet, there are very important models in this class, for instance, QCD with a $\theta-$term or at finite baryon density, whose solution might lead to an explanation of the strong CP problem and to the understanding of the rich phase structure expected for matter at high pressures. In condensed matter physics Haldane showed [2] that chains of quantum half-integer spins with antiferromagnetic interactions are related to the two-dimensional $O(3)$ nonlinear sigma model with a topological term at $\theta = \pi$, and conjectured that such model presents a second order phase transition at $\theta = \pi$, keeping its ground state CP symmetric. These are some of the reasons why a great effort is being invested in developing new algorithms, capable of dealing with complex actions.

For the particular case of $\theta-$vacuum systems, the partition function in the presence of a θ term is periodic and, conveniently normalized, can be decomposed in sectors of different topological charge n (or density of topological charge $x_n = n/V$), as

$$Z_V(\theta) = \sum_n p_V(n)\, e^{i\theta n} = \sum_n e^{-Vf_V(x_n)} e^{i\theta V x_n}, \tag{1}$$

which resembles the Fourier transform of the probability distribution function (p.d.f.) of the topological charge at $\theta = 0$. The probability of the topological sector n is therefore given by $p_V(n)$, and this quantity can, a priori, be measured from numerical simulations. Unfortunately, this is a very difficult task, for several reasons:

i. The precision in a numerical simulation is limited by statistical fluctuations. Thus the measurement of $p_V(n)$ suffers from errors.

ii. Small errors in $p_V(n)$ induce huge errors in the determination of $Z_V(\theta)$, as this quantity is exponentially small, $Z_V \approx e^{-V}$, due to the sign problem.

iii. Even if we were able to evaluate $p_V(n)$ with infinite accuracy, the terms on the sum (1) differs by many orders of magnitude (from 1 to e^{-V}).

In fact, the different groups that have tried to determine with high precision the p.d.f. of the topological charge either by standard simulations, or by more sophisticated methods (reweighting or multibinning techniques), have found artificial phase transitions in the $U(1)$ and CP^N models. The reason behind these ghost transitions is the flattening of the free energy for $\theta-$values larger than a certain threshold. In [3, 4], this threshold is roughly evaluated, and the flattening behaviour explained. The conclusion is clear: a reliable computation of the order parameter (or the free energy) for all values of θ from the direct measurement of the p.d.f. of the topological charge is not feasible due to the huge statistics required.

That is why other approaches [5, 6, 7, 8, 9, 10, 11, 12] (or at least, serious refinements of the standard approach) should be considered. In [13], a remarkable breakthrough was achieved, pushing the threshold of θ to its limit $\theta = \pi$. The method is based on the observation that, since all the coefficients entering in the right hand side of equation (1) are positive at purely imaginary values of θ, the free energy is given in the thermodynamic limit by the saddle point

$$f'(x) = h, \tag{2}$$

where $f(x)$ represents $f_V(x_n)$ as $V \to \infty$, and h stand for a purely imaginary θ field $\theta = -ih$.

Then, the function was fitted to a ratio of polynomials, and integrated analytically to obtain $f(x)$. This step is essentially different to what other groups proposed, and it solved the problem of the θ threshold in some systems. Finally, a multi-precision algorithm is used to calculate the partition function directly from (1), using the function $f(x)$.

It was demonstrated numerically in [13] that the errors in the reconstructed $f(x)$ using this method were highly correlated. This was a great advantage, for the errors, propagated to the exact free energy density, became almost constant, and these errors amounted to an irrelevant constant in the free energy. These ideas were successfully tested [13] in the one-dimensional Ising model and the two-dimensional $U(1)$ model, and the method was used to predict the behaviour of the CP^3 model. Furthermore, in reference [14] the continuum θ dependence of CP^9 –a confining and asymptotically free quantum field theory– was fully reconstructed. Data collapsed for different couplings within percent level and this evidence for scaling at non-zero θ is the strongest indication that the CP symmetry is spontaneously broken in the continuum, as predicted by the large N expansion.

The results were impressive by that time, solving completely the problem of the flattening of the order parameter beyond the critical value of θ. The key of this success was the aforementioned correlation among the errors: tests performed using the same method and adding an apparently negligible 0.1% uncorrelated random error to the measured free energy $f(x)$ led to disaster. Nonetheless, if the error was correlated, it could be as large as 50%, and the final result would be quite reasonable.

However, this method is not yet generally applicable. The flattening can appear –and in fact, does– whenever the behaviour of the order parameter is not monotonous. This seems to be a general rule. The flattening was first observed in a simple toy model which featured symmetry restoration at $\theta = \pi$,

$$f(\theta) = \ln(1 + A\cos\theta). \tag{3}$$

For this model, the order parameter vanishes only at $\theta = 0, \pi$

$$im(\theta) = \frac{A\sin\theta}{1 + A\cos\theta}, \tag{4}$$

but the method predicted an almost flat behaviour, slightly increasing, beyond the point $\theta = \frac{\pi}{2}$.

On the whole, although the method proposed in [13] represented a large improvement over what existed at that point, it was clear that another approach was necessary, and that is how the method described in the following section was created [1].

2 One-dimensional Ising model

The Ising model is the simplest model describing ferromagnets, but it is also a good theoretical laboratory to test new algorithms. It is easy to code efficiently on the computer, and simulations are very fast, allowing the generation of big statistics, even on large lattices. The one-dimensional model in a magnetic field is exactly soluble, which allows us to check our results against the exact solution. We can also identify in some sense magnetization and topological charge in this model, and regard an imaginary external magnetic field as a θ term in the action. Finally, from the numerical point of view, it is even more challenging[1] than other complex systems suffering from the sign problem, such as lattice QCD with a $\theta-$term, yet it remains more accessible. Therefore, it is a good idea to check the goodness of any algorithm in this toy model, prior to its application to more physically interesting systems.

The hamiltonian of the one-dimensional Ising model with nearest neighbours coupling J and external magnetic field B is

$$H\left(\{s_i\}, J, B\right) = -J \sum_i^N s_i s_{i+1} - B \sum_i^N s_i. \tag{5}$$

Defining reduced couplings $F = J/(KT), h = 2B/(KT)$, the density of free energy is given by

$$f\left(F, h\right) = F + \ln\left(\cosh\frac{h}{2} + \sqrt{e^{-4F} + \sinh^2\frac{h}{2}}\right), \tag{6}$$

where $f\left(F, h\right) = 1/V \ln Z$ represents the free energy. It is quite remarkable that the Ising model within an imaginary external field (i.e., for $h = -i\theta$ with $\theta \in \mathbb{R}$) is not properly defined with ferromagnetic couplings [27]. Setting $F > 0$ we find that the free energy (6) becomes undefined for certain values of θ, for the argument of the logarithm may vanish if $F > 0$. Hence, we will deal with the antiferromagnetic Ising model ($F < 0$) from now on.

In systems with an even number of spins, the quantity $\frac{M}{2} = \frac{1}{2}\sum_{j=1}^N s_j$ is an integer taking any value between $-N/2$ and $N/2$. From equation (6), the mean density of magnetization is

$$\langle m \rangle = \frac{\partial f}{\partial \frac{h}{2}} = \frac{\sinh\frac{h}{2}}{\sqrt{e^{-4F} + \sinh^2\frac{h}{2}}}. \tag{7}$$

Equation (7) for the magnetization is completely general, in particular it is valid for the case of a pure imaginary magnetic field $h = i\theta$. For $\theta = \pi$, the Z_2 symmetry is restored (the magnetic field amounts to a sign σ, depending on the 'topological charge' $M/2$ of the configuration $\sigma = e^{i\pi M/2}$; this sign is invariant under a Z_2 transformation). Then, the question is whether the Z_2 symmetry is spontaneously broken or not. Substituting $h \to i\theta$ in (7), we get

$$\langle m \rangle = \frac{i\sin\frac{\theta}{2}}{\sqrt{e^{-4F} - \sin^2\frac{\theta}{2}}}. \tag{8}$$

Thus the magnetization takes a non-zero expectation value for the one-dimensional Ising model at $\theta = \pi$, a fact that indicates spontaneous symmetry breaking (see fig. 1).

[1]As the following sections show, the phase diagram of the Ising model within an imaginary magnetic field is richer than the one expected for QCD in presence of a $\theta-$vacuum term.

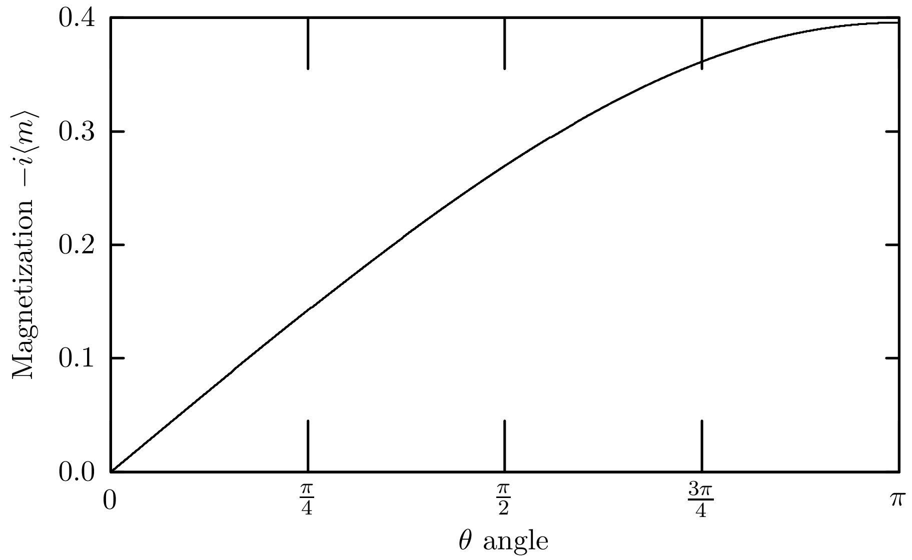

Figure 1: Magnetization density as a function of the θ angle for the one-dimensional Ising model. F was set to $F = -0.50$.

The Ising model in one dimension has a striking scaling property. Let us define the variable $z = \cosh\frac{h}{2}$, and compute the ratio $\frac{\langle m\rangle}{\tanh\frac{h}{2}}$:

$$y(z) = \frac{\langle m\rangle}{\tanh\frac{h}{2}} = \frac{\left(e^{-4F}-1\right)^{-\frac{1}{2}} z}{\sqrt{\left(e^{-4F}-1\right)^{-1} z^2 + 1}} \tag{9}$$

Therefore $y(z)$ depends on z and F only through the combination $\left(e^{-4F}-1\right)^{-\frac{1}{2}} z$. Due to this simplified dependency on F and h, the transformation

$$y_\lambda(z) = y\left(e^{\frac{\lambda}{2}} z\right) \tag{10}$$

with $\lambda \in \mathbb{R}$ is equivalent to a change in the reduced coupling F, or in the temperature of the model. The interesting point here is the fact that for negative values of λ, this transformation can take the variable $z = \cosh\frac{h}{2}$ to the range $0 < z < 1$, therefore $z = \cos\frac{\theta}{2}$, corresponding to an imaginary field. This means that we can measure $y(z)$ for imaginary values of the magnetic field by mean of numerical simulations at real values of h, which are free from the sign problem.

In order to check if a similar scaling property still holds for other systems, let us assume that $y(z, F) = y(g(F) z)$, then

$$\frac{\frac{\partial y}{\partial F}}{\frac{\partial y}{\partial z}} = \frac{g'(F) z}{g(F)} \tag{11}$$

To have scaling, the ratio $\frac{\partial y}{\partial F}/z\frac{\partial y}{\partial z}$ should be independent of h.

For the one-dimensional Ising model the simulations exhibit a constant ratio over a large range of fields h (see Fig. 2).

Unfortunately, this property is exclusive of the one-dimensional case. For two dimensions the ratio shows a slightly dependence on the reduced magnetic field. For three dimensions, the dependence becomes a bit more pronounced. The peak in Fig. 3 is produced by the antiferromagnetic-ferromagnetic phase transition[2].

[2]The antiferromagnetic Ising model displays, for strong enough couplings, a phase transition at non-zero external magnetic field : the spin-coupling tries to put the system in an antiferromagnetic state, whereas the external field tries to order the spins in a ferromagnetic fashion. As the value of the external field increases, the ferromagnetic behaviour takes over.

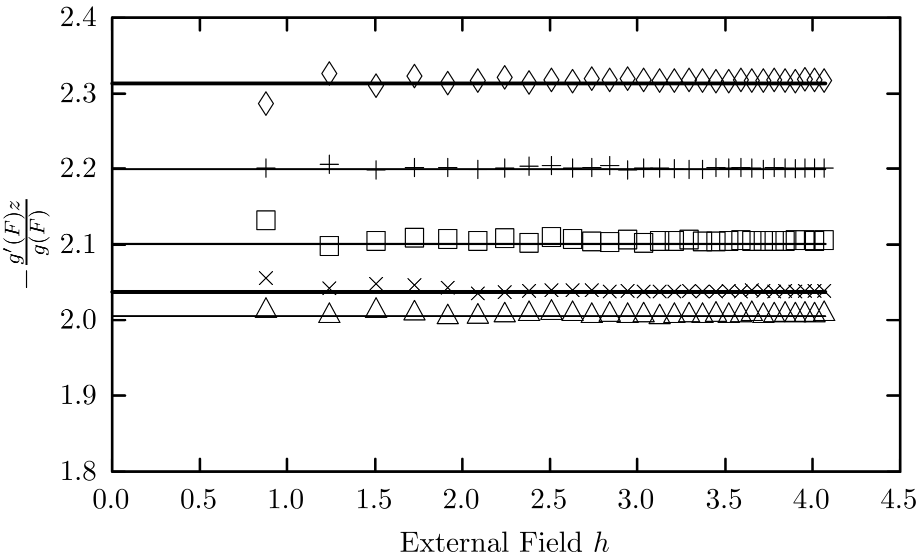

Figure 2: Ising's scaling check along formula (11). The continuous lines represent the analytical result, while the crosses stand for the numerical data. We performed short simulations (only ~ 100000 iterations) for several values of F in a $L = 100$ lattice. Errors are smaller than symbols.

In any case, the dependence on the external field for these two models is mild for small values of the field h, far from the transition point, and large values of $|F|$ (for low temperatures). We will see later that this property becomes very relevant when dealing with asymptotically free theories.

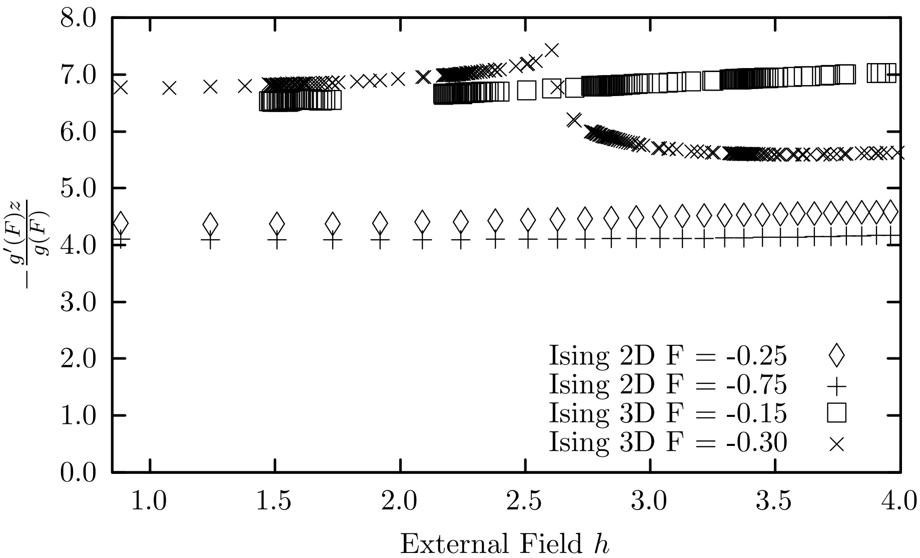

Figure 3: Ising's results in 2D and 3D. The scaling is approximate in 2D and 3D for low values of the field. The statistics of the simulations are 100000 iterations, and the lattice lengths are, for 2D $L = 50$ and for 3D $L = 25$. Errors are smaller than symbols.

3 Computing the order parameter for imaginary magnetic fields

Although the exact scaling property is absent in higher dimensions, we can still take advantage from the methodology it suggests. For the one-dimensional case, a measurement of

the order parameter produced at the point (F, z) is equivalent to a measurement done at (F', z') if the following relationship holds

$$g(F)\,z = g(F')\,z',$$

$$g(F) = \left(e^{-4F} - 1\right)^{\frac{1}{2}}. \tag{12}$$

This way, and choosing carefully the value of F, a simulation performed at a real value of the reduced magnetic field $z \geq 1$ is equivalent to another simulation performed at imaginary values of h (where $z < 1$).

The procedure to find out the order parameter at imaginary values of the reduced magnetic field relies on scaling transformations [1]. We define the function $y_\lambda(z)$ as

$$y_\lambda(z) = y\left(e^{\frac{\lambda}{2}} z\right). \tag{13}$$

For negative values of λ, the function $y_\lambda(z)$ allows us to calculate the order parameter $\left(\tanh \frac{h}{2}\, y(z)\right)$ below the threshold $z = 1$. If $y(z)$ is non-vanishing for any positive z[3], then we can plot y_λ/y against y. Furthermore, in the case that y_λ/y is a smooth function of y close to the origin, then we can rely on a simple extrapolation to $y = 0$. Of course, a smooth behaviour of y_λ/y can not be taken for granted; however no violations of this rule have been found in the exactly solvable models.

The behaviour of the model at $\theta = \pi$ can be ascertained from this extrapolation. At this θ the model has the same Z_2 symmetry as in the absence of field. We define a critical exponent γ_λ

$$\gamma_\lambda = \frac{2}{\lambda} \ln\left(\frac{y_\lambda}{y}\right) \tag{14}$$

As $z \to 0$, the order parameter $\tan\frac{\theta}{2}\, y\left(\cos\frac{\theta}{2}\right)$ behaves as $(\pi - \theta)^{\gamma_\lambda - 1}$. Therefore, a value of $\gamma_\lambda = 1$ implies spontaneous symmetry breaking at $\theta = \pi$. A value between $1 < \gamma_\lambda < 2$ signals a second order phase transition, and the corresponding susceptibility diverges. Finally, if $\gamma_\lambda = 2$, the symmetry is realized (at least for the selected order parameter), there is no phase transition and the free energy is analytic at $\theta = \pi$.[4]

We can take the information contained in the quotient $\frac{y_\lambda}{y}(y)$, and calculate the order parameter for any value of the imaginary reduced magnetic field $h = -i\theta$ through an iterative procedure [1]. The outline of the procedure is the following:

i. Beginning from a point $y(z_i) = y_i$, we find the value y_{i+1} such that $y_\lambda = y_i$. By definition, $y_{i+1} = y\left(e^{\frac{-\lambda}{2}} z_i\right)$.

ii. Replace y_i by y_{i+1}, to obtain $y_{i+2} = y\left(e^{-\lambda} z_i\right)$.

The procedure is repeated until enough values of y are know for $z < 1$ (see Fig. 4). This method can be used for any model, as long as our assumptions of smoothness and absence of singular behaviour are verified during the numerical computations. Indeed the reliability of our approach in practical aplications is better when the following two points are well realized:

a. $y(z)$ takes small values for values of z of order 1.

b. The dependence on y of the functions y_λ/y and γ_λ is soft enough to allow a reliable extrapolation.

In the one-dimensional model these two properties are realized in the low temperature regime (see equation 9 and Fig. 5), but the two and three-dimensional models, notwithstanding they do not verify a perfect scaling law as in the one-dimensional case, they also show a

[3] Even though the possibility of a vanishing $y(z)$ for some value $z > 0$ can not be excluded completely, it does not happen for any of the analitically solvable models we know.

[4] Other possibilities are allowed, for instance, any $\gamma_\lambda > 1, \quad \gamma_\lambda \in \mathbb{N}$ leads to symmetry realization for the order parameter at $\theta = \pi$ and to an analytic free energy. If γ_λ lies between two natural numbers, $p < \gamma_\lambda < q, \quad p, q \in \mathbb{N}$, then a transition of order q takes place.

very good behaviour (see Figs. 7, 8). Indeed the relevant feature, at least in what concerns point a, is that, at low temperatures, the magnetic susceptibility at small values of the real external magnetic field h, which is essentially $y(z)$, takes small values; and this is also true for any dimension. In the more interesting case of asymptotically free models, the analogue of the magnetic susceptibility is the topological susceptibility, and it is well known that topological structures are very suppresed near the continuum limit. Therefore, and on qualitative grounds, we expect a much better implementation of our method in the low temperature regime of the Ising model and near the continuum limit of asymptotically free theories. A check of this statement for the Ising model is the content of this article, and concerning asymptotically free models, the method was successfuly applied to the analysis of the continuum $\theta-$dependence of CP^9 [14], showing a very good realization of points a and b. In the more general cases we should find out whether the model complies with these two points or not, and pleasant surprises are not excluded. Indeed, we checked in [28] that the conditions for the aplication of our approach to CP^1 also hold, and this allowed us to verify the Haldane conjecture and the relevant universality class of the non-linear $O(3)$ σ-model in two dimensions.

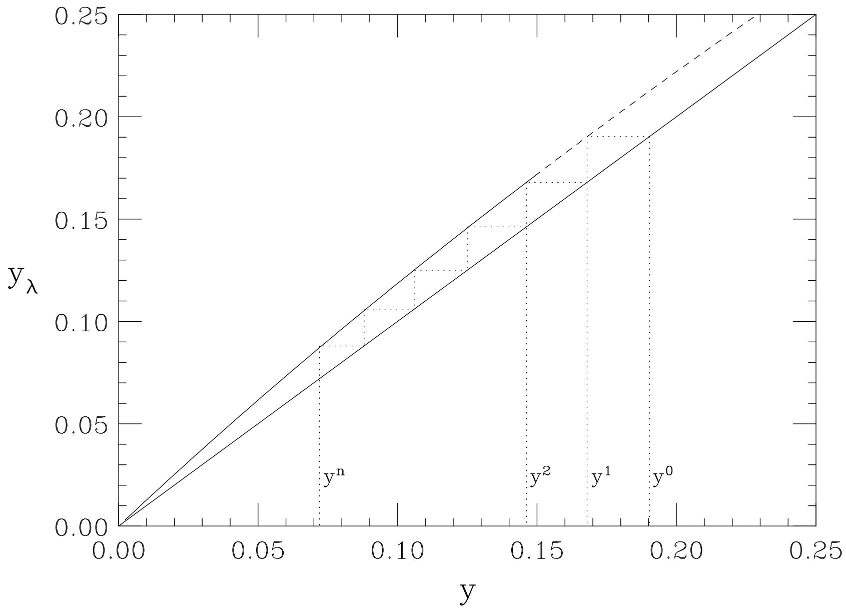

Figure 4: Iterative method used to compute the different values of $y(z)$. y_λ is ploted as a function of y using a dashed line in the region where direct measurements are available, and a continuous line in the extrapolated region. The straight continuous line represents $y_\lambda = y$.

4 Numerical results

The first thing we did was to test the method in the one-dimensional Ising model, and we checked the results against (8). The simulations were performed at a fixed volume, $N = 1000$ spins, and fixed reduced coupling $F = -2.0$. As the one-dimensional Ising model has no phase transitions, and furthermore enjoys the exact scaling property, there is no point in checking the method for several values of the reduced coupling. The parameter we varied was the reduced magnetic field h. As the simulations were quite fast, we could obtain data for many values of h with large statistics. In fact, for each point in the plots we performed 10^7 metropolis iterations. In order to reduce autocorrelations, we performed at each iteration two sweeps over the lattice, proposing metropolis changes in the spins. The plots for the

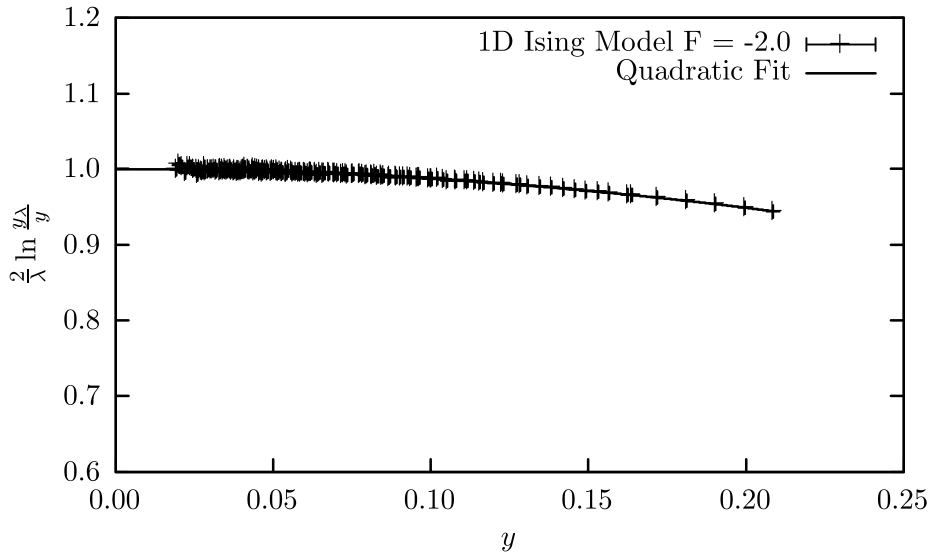

Figure 5: Calculation of the critical exponent γ_λ. The crosses correspond to the numerical simulation data, whereas the line is a quadratic fit. The extrapolation to zero seems quite reliable, as the function is smooth enough. Errors are smaller than symbols.

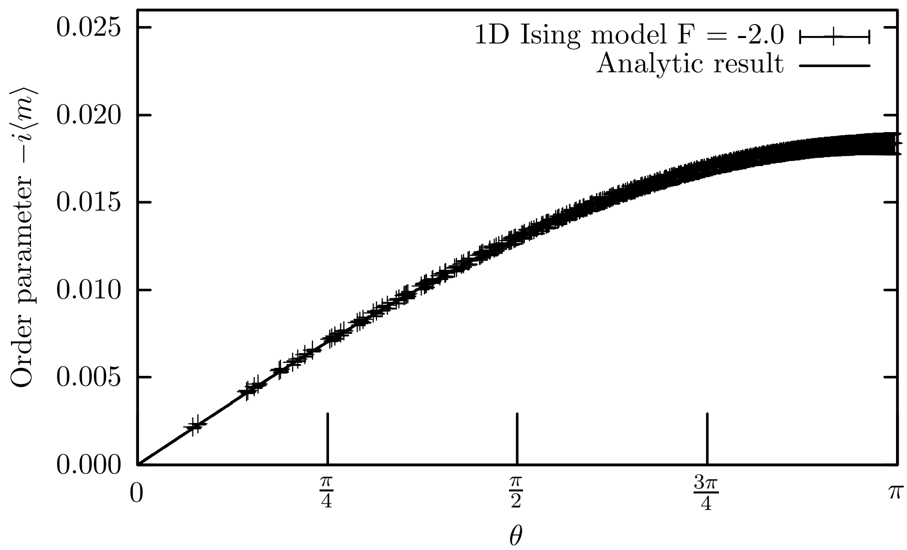

Figure 6: Order parameter as a function of θ. The non-zero value of the order parameter marks the spontaneous breaking of the Z_2 symmetry at $\theta = \pi$.

critical exponent and the order parameter are shown in Figs. 5 and 6. Our result for the critical exponent from the fit in fig. 5 is

$$\gamma_\lambda = 0.99980 \pm 0.00008,$$

which agrees with the analytical result.

Then we simulated higher dimensional models, expecting to see departures from this behaviour, as these models feature phase transitions between ordered (antiferromagnetic) and disordered phases. The two-dimensional simulations were done in a 100^2 lattice, after 100000 termalization sweeps. We spent 5000000 steps to measure each point accurately. The three-dimensional case, on the other hand, used a 50^3 volume, and measured each point for 2500000 steps after 100000 steps of thermalization. The results showed the expected departure in the behaviour. Our result for the critical exponent $\gamma_\lambda \approx 2$ reveals a vanishing order parameter at $\theta = \pi$ in the ordered phase ($F = -1.50$ for $2D$ and $F = -1.00$ for $3D$),

as shown in Figs. 7, 8, 9 [5].

$$\gamma_\lambda^{2D} = 1.9997 \pm 0.0002$$
$$\gamma_\lambda^{3D} = 1.9998 \pm 0.0002$$

We can confirm this facts by plotting the order parameter against θ, as it is done in Fig. 10 and 11.

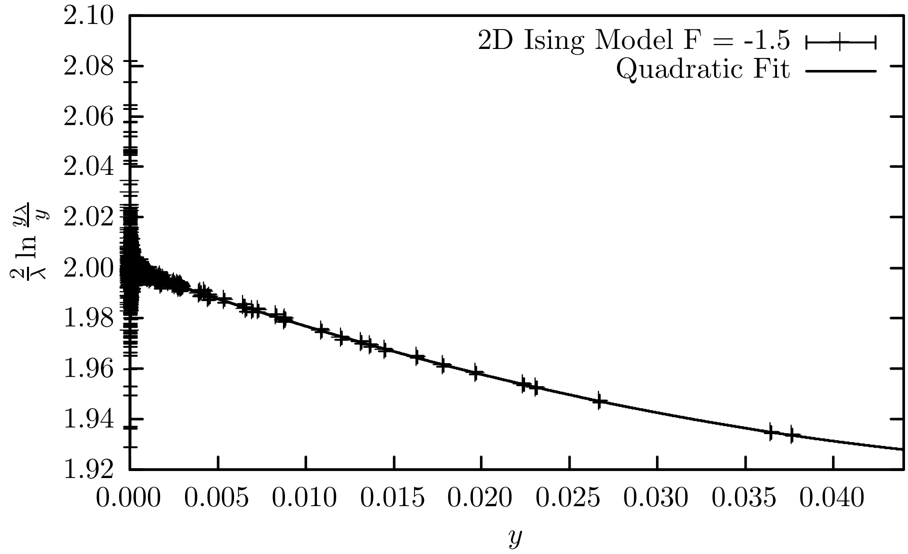

Figure 7: Calculation of the critical exponent γ_λ in the ordered phase of the two-dimensional model. The pluses correspond to the numerical simulation data, whereas the line is a cuadratic fit. Errors are much smaller than symbols, except for the points lying close to the origin.

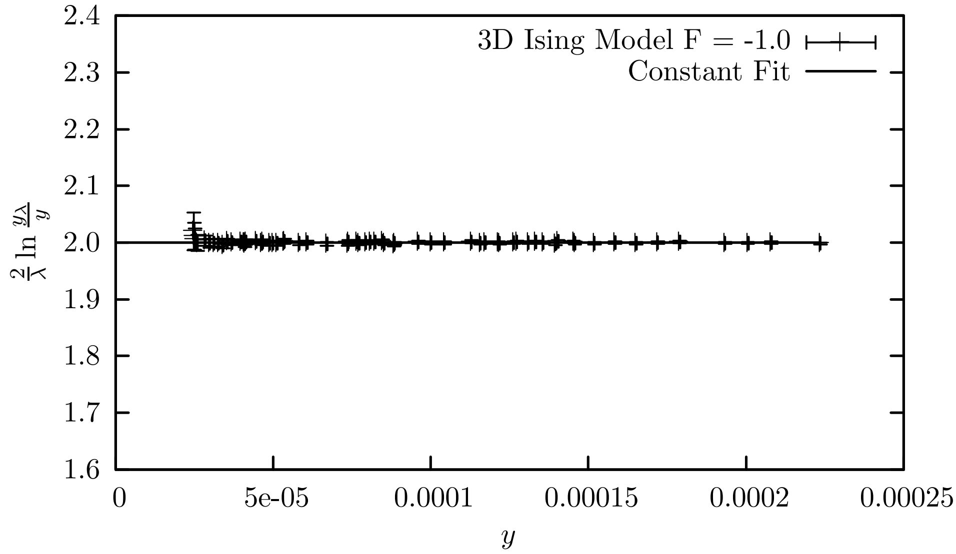

Figure 8: Calculation of the critical exponent γ_λ in the ordered phase of the three-dimensional model. The pluses correspond to the numerical simulation data, whereas the line is a constant fit. Errors are much smaller than symbols, except for the points lying close to the origin.

The disordered phase revealed a caveat of this method, as it was impossible for us to extrapolate the function $\frac{y_\lambda}{y}(y)$ to zero. The reason is simple: at small values of F, y and y_λ approach unity, for at vanishing F we recover the paramagnetic Langevin solution

[5] Actually the Z_2 symmetry is spontaneously broken, for the staggered magnetization $m_S \neq 0$ [29]. This point will be clarified in the mean-field approximation.

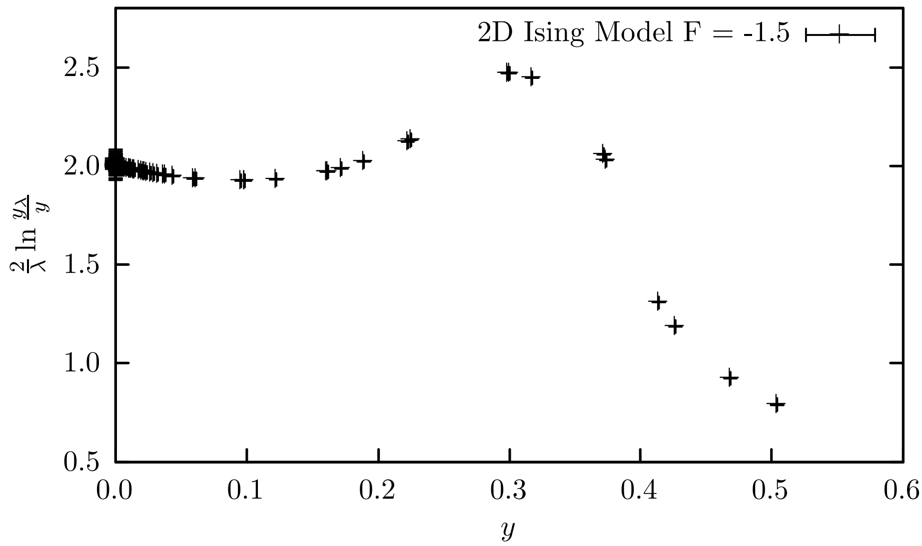

Figure 9: Due to the peaked behaviour of the quotient y_λ/y around $y = 0.3$, the extrapolation to zero required many simulations at small values of the magnetic field. Errors are much smaller than symbols, except for the points lying close to the origin.

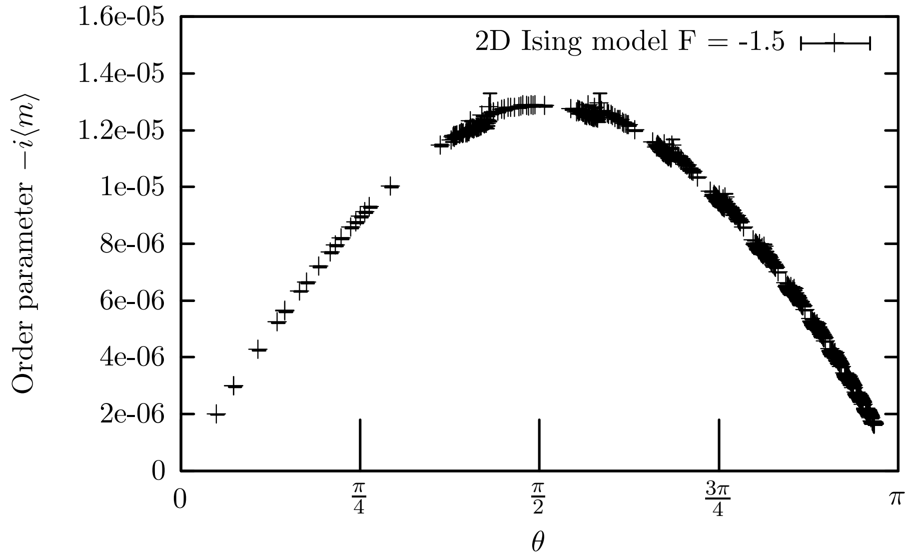

Figure 10: Order parameter as a function of θ in the ordered phase of the two-dimensional model. It vanishes at $\theta = \pi$.

$m = \tan\frac{\theta}{2}$ and $y = 1$. The smaller the value of F, the greater the gap between zero and our data becomes, and at some point, the extrapolation is not reliable any more, and the results depend strongly on the fitting function used. An example can be seen in Fig. 12, where the data for the two-dimensional model at $F = -0.40$ are plotted. In this case, we are too far from zero to find out accurately the critical exponent, and the value of F could not be lowered much more, for the transition to the ordered phase is known to happen at $F \sim -0.44$. In Fig. 13 a similar example is shown for the ordered phase in the three-dimensional model, but this time a tentative extrapolation could be done, casting a reliable result.

These examples show how this method works fine when the antiferromagnetic couplings are strong enough. In general, as discussed at the end of the previous section, the method performs well in the low temperature regime od the Ising model and for asymptotically free theories, whose continuum limit lie in the region of weak coupling. In this region, the density

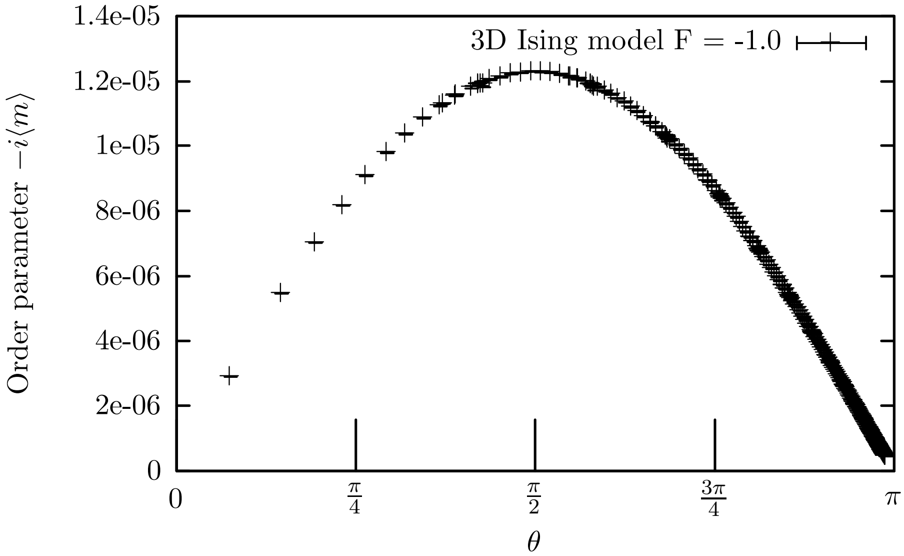

Figure 11: Order parameter as a function of θ in the ordered phase of the three-dimensional model. As in its two-dimensional counterpart, it vanishes at $\theta = \pi$. Errors are smaller than symbols.

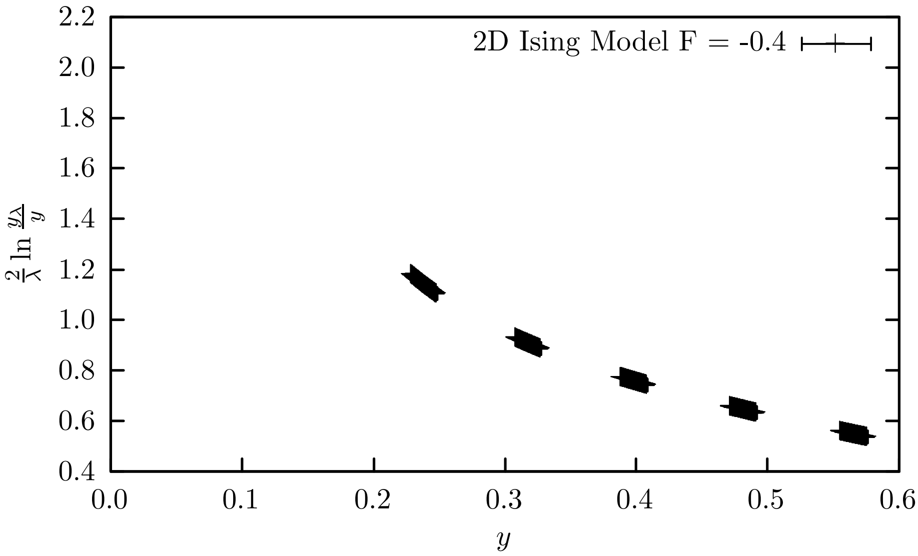

Figure 12: Failed calculation of the critical exponent γ_λ in the disordered phase for the two dimensional model. Our data is so far from the $y = 0$ axis, that an extrapolation can not be used to find out the value of γ_λ. A peak for lower values of y, as the one appearing in Fig. 9, cannot be discarded 'a priori'. Errors are much smaller than symbols.

of topological structures is strongly suppressed. Thus the order parameter and $y(z)$ take small values, making the plot $\frac{y_\lambda}{y}(y)$ easily extrapolable to zero. In the particular case of the antiferromagnetic Ising model, large values of $|F|$ ensure a small magnetic susceptibility. A high value of the dimension also helps, for instance, the three-dimensional model requires a lower value of the coupling than the two-dimensional case to make a reliable extrapolation of $\frac{y_\lambda}{y}(y)$ to $y \to 0$, for each spin is affected by a higher number of neighbours.

As this method failed to deliver interesting results in the disordered phase, we tried a different approach: we expected naively that the two-dimensional model resemble the one-dimensional model at low values of the coupling. Since the p.d.f. method worked well for the one-dimensional case [13], it made sense that we applied it to the present scenario. What we found is an unstable behaviour: sometimes the method seems to predict the phase transition, in the sense that at finite volume there is not true phase transition, and an abrupt

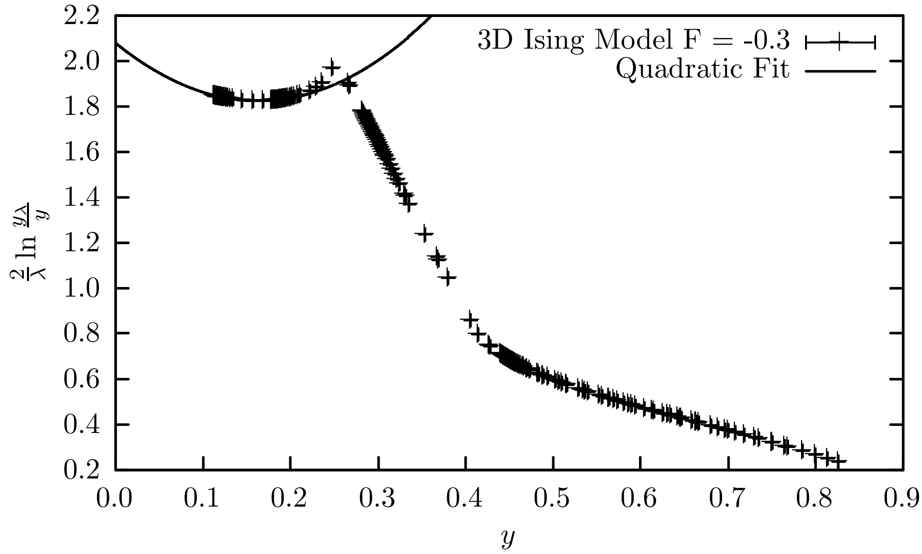

Figure 13: Another calculation of the critical exponent γ_λ in the ordered phase $F = -0.3$ for the three-dimensional model. Our data approaches the $y = 0$ axis enough to try an extrapolation, but the result suffers from much larger errors than in the $F = -1.0$ case. Here $\gamma_\lambda = 2.079 \pm 0.003$, and the measurement errors are much smaller than symbols.

modification in the order parameter, linking the two expected behaviours, should happen. This is what we observe in one of the data sets of Fig. 14. Nonetheless, if a slightly different set of points is taken to fit the saddle point equation (2), the resulting data show a sharp departure from the expected behaviour at some θ.

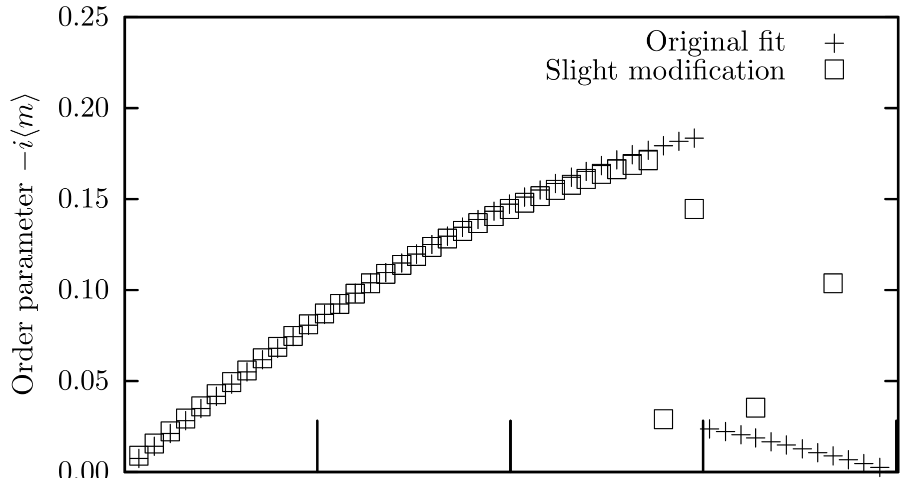

Figure 14: Failed calculation of the order parameter in the disordered phase using the improved p.d.f. method described at the beginning of this paper. In the first case, the points seem to predict a phase transition at $\theta \sim 2.35$, whereas in the second case the points depart sharply from a smooth function and never come back. The only difference between fits was the number of points used: in the second case, only half of the points (the closest to the origin) were used. Other modifications in the fitting procedures indicate us that the transition point is not stable. This might indicate either a failure in the fitting function, or a phase transition, and the impossibility for the method to precise the transition point, unless a perfect ansatz is made. Errors were not estimated.

There are two possible explanations to this behaviour: either the fitting function selected is wrong, or there is some hidden phenomenon we are overlooking. The fitting function used

was an odd quotient of polynomials

$$\frac{ax^3 - x}{cx^2 - b}$$

which should account well for the behaviour of the order parameter, given the assumption that it is similar to the one-dimensional case. The addition of more terms to the fit did not do much to improve the result, hence this possibility was discarded.

The existence of a phase transition in the middle, however, was an interesting option. Indeed, the two-dimensional model in the presence of a θ term was solved exactly at the point $\theta = \pi$ almost sixty years ago by Yang and Lee in [29], and reviewed again in [30]. In those papers, a phase diagram was proposed were the antiferromagnetic model always stayed in an ordered phase at any non-zero value of F. Since the system is in a disordered state for low F's and zero field, some phase transition has to occur in the middle. Thence, the failure of the p.d.f. method should be due to a poor ansatz for the fitting function, caused by the presence of a phase transition at some θ_c.

The fact that the results for the two- and three-dimensional models are qualitatively the same in the ordered phase, makes us wonder whether this behaviour changes for some value of the dimension $D > 3$. Moreover, the behaviour of this model in the disordered phase is unknown to us. That is why we decided to carry out a mean-field approximation of the model, and compute the critical exponent γ_λ. As we know, mean-field results for other critical exponents are exact for the n-dimensional ferromagnetic Ising model, provided that $n \geq 4$. Thus we expect that, if the mean-field result for γ_λ is the same to that of the two- and the three-dimensional Ising model, then $\gamma_\lambda = 2$ for any value of the dimension.

5 Mean-field calculation

In antiferromagnetic compounds the spin-alignment pattern is staggered, hence, in order to define the mean-field version of the antiferromagnetic Ising model, we should divide the lattice in two sublattices, and define a coupling among spins whose sign depends on whether these two spins are on the same sublattice or not. For spins belonging to the same lattice, the coupling should be ferromagnetic ($J > 0$), but for spins belonging to different sublattices, the coupling should favour antiparallel ordering ($-J < 0$), according to the antiferromagnetic nature of the system. Therefore, two different mean-fields should appear, $\langle s_i \rangle_{i \in S_1} = m_1$ and $\langle s_i \rangle_{i \in S_2} = m_2$, referring to each one of the different sublattices.

A reasonable mean field hamiltonian compatible with these requirements is [6]

$$H\left(J, B, \{s_i\}\right) = -\frac{J}{N}\left(\sum_{i \in S_1} s_i - \sum_{j \in S_2} s_j\right)^2 - B_1 \sum_{i \in S_1} s_i - B_2 \sum_{j \in S_2} s_j. \tag{15}$$

We define as before $h_i = \frac{2B_i}{KT}$ (for each sublattice $i = 1, 2$) and $F = \frac{J}{KT}$, and the usual and the staggered magnetizations, $m = m_1 + m_2$, $m_S = m_1 - m_2$. We are interested in the model for imaginary values of the field, $h \to i\theta$. Using standard saddle point techniques (see appendix A for details) we obtain the mean field equations:

$$m = \frac{1}{2} \frac{i \sin\theta}{\cosh^2(2|F| m_S) - \sin^2 \frac{\theta}{2}}, \tag{16}$$

$$m_S = \frac{1}{2} \frac{\sinh(4|F| m_S)}{\cosh^2(2|F| m_S) - \sin^2 \frac{\theta}{2}}. \tag{17}$$

An analysis of these equations shows that for low values of F there's only one solution, $m_S = 0$, corresponding to a paramagnetic phase. For values over a certain F_c the situation

[6] Of course other mean-field approaches could be used, but we expect to obtain the same qualitative picture for the phase diagram. For example, a calculation in the scheme of [31] produces similar results, and more importantly the same value for γ_λ as the one in our calculation.

changes and two new symmetric solutions appear, which are in fact the physically relevant ones. From the saddle point equations, (30) and (31), F_c can be obtained as a function of θ:

$$2F_c = \cos^2 \frac{\theta_c}{2}. \tag{18}$$

The phase diagram of the system in the F-θ plane is shown in Fig. 15, There is a second

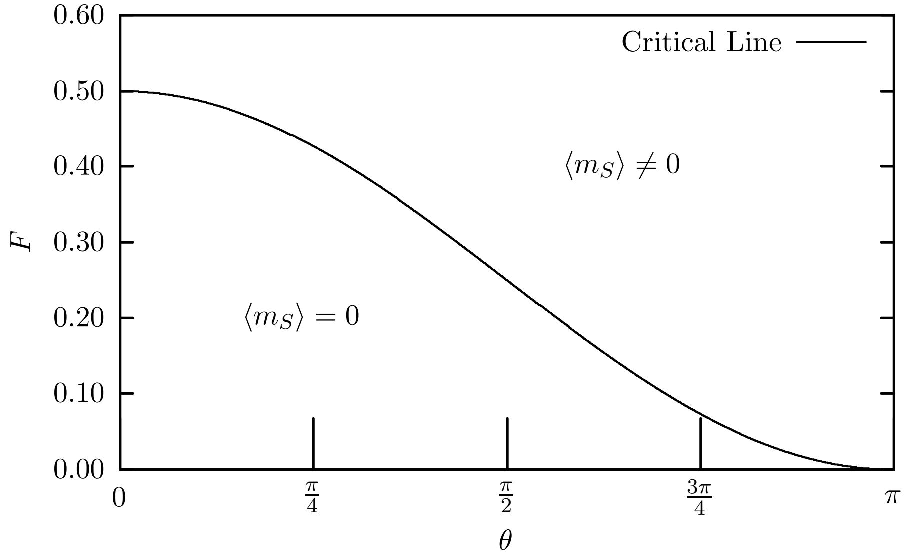

Figure 15: Phase diagram of the mean-field approximation to the antiferromagnetic Ising model in the $F-\theta$ plane.

order phase transition at the critical line (18). As $\theta \to \pi$ the paramagnetic phase narrows, until it is reduced to the single point $F = 0$ at $\theta = \pi$. The staggered phase (with antiparallel spin ordering $m_S \neq 0$ and $F > \frac{\cos^2 \frac{\theta}{2}}{2}$) on the other hand features Z_2 spontaneous symmetry breaking at $\theta = \pi$, as equation 17 shows. The fact that this model features a phase transition at non-zero values of the external field is quite remarkable. This kind of transitions would never appear in a ferromagnetic model within a real external magnetic field, as the external field and the spin coupling work in the same direction: parallel spin alignment. On the contrary, in the antiferromagnetic case, the introduction of a real external field produces frustration, whose origin comes from the competition of the spin coupling, trying to move the spins towards an antiparallel configuration, and the external field, favouring a completely parallel structure. What is remarkable of these results is the fact that in the antiferromagnetic case an imaginary magnetic field, strong enough, is able to move the system from the paramagnetic phase to a phase with antipararell ordering.

All the magnetizations are continuous functions, but the staggered susceptibility χ_S diverges, as usually happens in a second order phase transition. The *topological*[7] susceptibility χ_T, on the other hand, displays a gap at the critical line. The computation (see Appendix A) gives the result

$$\Delta\chi_T = \lim_{\theta \to \theta_c^+} \chi_T - \lim_{\theta \to \theta_c^-} \chi_T = \frac{3}{4\,|F|} \frac{2\,|F| - 1}{4\,|F| - 3}. \tag{19}$$

Finally, the critical exponent γ_λ for this mean-field theory can be calculated, to see if it coincides with that obtained in simulations. In order to do so, we expand m in the neighbourhood of $\theta = \pi$

$$m(\theta) \sim m(\pi) + \left.\frac{\partial m}{\partial \theta}\right|_{\theta=\pi} (\pi - \theta) + \left.\frac{\partial^2 m}{\partial \theta^2}\right|_{\theta=\pi} (\pi - \theta)^2 + \ldots \tag{20}$$

[7]Topological in the sense that $M/2$ is a quantized charge, $m/2$ is its associated charge density, and χ_T the susceptibility.

If γ_λ is not natural number, we expect the first non-zero derivative to diverge. On the contrary, if γ_λ is a natural number, the order of the first non-vanishing derivative will give us the critical exponent. Taking derivatives

$$\left.\frac{\partial m}{\partial \theta}\right|_{\theta=\pi} = \frac{i}{2}\frac{\left(2\cos^2\theta - 1\right)\cosh^2\left(2\left|F\right| m_S\right) + 1 - \cos^2\frac{\theta}{2}}{\left(\cosh^2\left(2\left|F\right| m_S\right) - \sin^2\frac{\theta}{2}\right)^2} -$$

$$\left. - \frac{i}{2}\frac{2\left|F\right|\sin\theta\sinh\left(4\left|F\right| m_S\right)\left.\frac{dm_S}{d\theta}\right|_{\theta=\pi}}{\left(\cosh^2\left(2\left|F\right| m_S\right) - \sin^2\frac{\theta}{2}\right)^2}\right|_{\theta=\pi} =$$

$$= -\frac{i}{2}\left[\frac{1}{\sinh^2\left(2\left|F\right| m_S\right)} + \frac{2\left|F\right|\sin\theta\sinh\left(4\left|F\right| m_S\right)\left.\frac{dm_S}{d\theta}\right|_{\theta=\pi}}{\sinh^4\left(2\left|F\right| m_S\right)}\right] \tag{21}$$

The first term on the r.h.s. of (5) does not diverge since m_S is not vanishing as $\theta \to \pi$. The second term is proportional to

$$\lim_{\theta\to\pi}\frac{dm_S}{d\theta}\sin\theta.$$

After a tedious calculation, it can be shown that it vanishes, therefore

$$m\left(\theta\right) \sim i\frac{\pi - \theta}{2\sinh^2\left(2\left|F\right| m_s\right)} \sim K\left(\pi - \theta\right), \tag{22}$$

with K a non-zero constant. The magnetization behaves as $(\pi - \theta)^{\gamma_\lambda - 1}$ in the neighbourhood of $\theta = \pi$. Thence, for mean-field antiferromagnetic theory $\gamma_\lambda = 2$ for $F \neq 0$. For $F = 0$ $\gamma_\lambda = 0$ and the magnetization diverges as $\tan\frac{\theta}{2}$ when $\theta \to \pi$.

Since mean-field theory works better in high dimensional systems (it reproduces all the critical exponents exactly for the ferromagnetic Ising model in dimension 4 and above), and the exponent γ_λ seems to have settled in $\gamma_\lambda = 2$ for the two- and three-dimensional models, and for the mean-field approximation, we expect this result to hold for any dimension of the system. This is not a proof, but in fact, it would be very remarkable if the behaviour of the antiferromagnetic Ising model in a higher dimension departed from $\gamma_\lambda = 2$.

6 Conclusions

Although the aim behind this investigation of the antiferromagnetic Ising model is to test our techniques for a future application to QCD in presence of a θ term, the results obtained through this work deserve attention on their own merit. Using the method described in section 3, the order parameter for the Z_2 symmetry can be calculated for any value of θ, and although there are some regions of the phase diagram where the method does not work well (high temperature regime), it provided us with enough information to make an educated guess on the phase diagram of the theory.

Our guess was later confirmed by a mean-field calculation, which shares many properties with the original model. The results of [29] and [30] supplied the remaining information for the two-dimensional case. In the end, we were able to reconstruct qualitatively the whole phase diagram of the theory for two-dimensions, and although we did not pursue to solve the model for higher dimensions, the mean-field calculations, and the fact that the behaviour for the two- and the three-dimensional models is the same for large values of F, give us strong indications that this phase diagram is qualitatively valid for any dimension of the model larger than one. The one-dimensional model is an exceptional case in which only one phase appears with spontaneous magnetization at $\theta = \pi$. On the contrary for $d = 2, 3$ our numerical simulations show a density of magnetization that continuously vanishes at $\theta = \pi$ at low temperatures, and the mean field calculation strongly suggests that this result holds for any temperature and any larger dimension. However this does not mean that the Z_2 symmetry of the model at $\theta = \pi$ is realized in the ground state since the mean field calculation shows a non vanishing value of the staggered magnetization at $\theta = \pi$.

Indeed there is a region of non-vanishing measure in the $F-\theta$ plane, including the $\theta=\pi$ line, where the staggered magnetization does not vanish and the saddle point equation (17) shows two symmetric solutions for this quantity. In all this phase translational invariance is spontaneously broken and in the $\theta=\pi$ line parity is also spontaneously broken.

The method only has two caveats:

i. It does not work properly (and can give wrong results) if there is a phase transition for some $\theta<\pi$.

ii. For small absolute values of the coupling F (high temperatures) the required extrapolations are not feasible.

Fortunately, the standard wisdom on QCD, based on reasonable assumptions, expects only one phase transitions at $\theta=\pi$ [32], and QCD is an asymptotically free theory, thus its continuum limit lies, as discussed in section 3, in the "low temperature" regime where our approach works well. Therefore this method has become the perfect candidate to perform simulations of QCD with a θ term, which might provide precious information concerning the strong CP problem.

A final remark on the antiferromagnetic Ising model at $\theta=\pi$ is pertinent. By using polymerization techniques an algorithm able to simulate the model at $\theta=\pi$ and free from the sign problem can be developed, and it could be useful to test if the mean field predictions reported here are verified for any dimension larger than 1 and any temperature at $\theta=\pi$.

7 Acknowledgments

This work has been partially supported by MICINN (grant FPA2009-09638 and grant FPA2008-01732), DGIID-DGA (grant2007-E24/2) and by the European Union under Grant Agreement number PITN-GA-2009-238353 (ITN STRONGnet). E. Follana is supported by MICINN through the Ramón y Cajal program, and A. Vaquero was supported by MICINN through the FPU program.

A Mean field model

The hamiltonian of the mean-field model is:

$$H\left(J,B,\{s_i\}\right)=-\frac{J}{N}\left(\sum_{i\in S_1}s_i-\sum_{j\in S_2}s_j\right)^2-B_1\sum_{i\in S_1}s_i-B_2\sum_{j\in S_2}s_j. \tag{23}$$

where we have assummed that an independent field B_i acts on each sublattice $i=1,2$. This modification will allow us to compute separately m_1 and m_2 once we have obtained the free energy; but of course, for the case of an uniform external field we shuld set $B=B_1=B_2$ at the end of the calculation.

We define as before $h_i=\frac{2B_i}{KT}$, $\quad i=1,2$ and $F=\frac{J}{KT}$, and the usual and the staggered magnetizations, $m=m_1+m_2$, $m_S=m_1-m_2$. The partition function

$$Z\left(F,h\right)=\sum_{\{s_i\}}e^{\frac{F}{N}\left(\sum\limits_{i\in S_1}s_i-\sum\limits_{j\in S_2}s_j\right)^2+\frac{h_1}{2}\sum\limits_{i\in S_1}s_i+\frac{h_2}{2}\sum\limits_{j\in S_2}s_j} \tag{24}$$

can be summed up by applying the Hubbard-Stratonovich identity to linearize the exponent

$$Z\left(F,h\right)=\frac{1}{\pi^{\frac{1}{2}}}\int_{-\infty}^{\infty}\sum_{\{s_i\}}e^{-x^2+\left[2x\frac{|F|^{\frac{1}{2}}}{N^{\frac{1}{2}}}+h_1\right]\sum\limits_{i\in S_1}s_i-\left[2x\frac{|F|^{\frac{1}{2}}}{N^{\frac{1}{2}}}-h_2\right]\sum\limits_{j\in S_2}s_j}dx. \tag{25}$$

At this point we see that the introduction of the θ term through the transformations

$$h_1\to i\theta_1,\qquad h_2\to i\theta_2,$$

render the hyperbolic cosines complex. The $\frac{1}{2}$ factor allows us to define properly the quantized number $\frac{M}{2}$. The integrand factorizes, as there is no spin-spin interaction

$$Z(F,h) = \frac{2^N}{\pi^{\frac{1}{2}}} \int_{-\infty}^{\infty} e^{-x^2} \left[\cosh\left(2x\frac{|F|^{\frac{1}{2}}}{N^{\frac{1}{2}}} + i\frac{\theta_1}{2} \right) \times \right.$$
$$\left. \cosh\left(2x\frac{|F|^{\frac{1}{2}}}{N^{\frac{1}{2}}} - i\frac{\theta_2}{2} \right) \right]^{\frac{N}{2}} dx. \tag{26}$$

Now we bring the transformation

$$\begin{array}{rcl} x & \to & N^{\frac{1}{2}} y \\ dx & \to & N^{\frac{1}{2}} dy \end{array}$$

so (A) becomes

$$Z(F,h) = \frac{2^N N^{\frac{1}{2}}}{\pi^{\frac{1}{2}}} \int_{-\infty}^{\infty} \left[e^{-y^2 + \frac{1}{2}\ln\left[\cosh\left(2|F|^{\frac{1}{2}}y + i\frac{\theta_1}{2}\right)\cosh\left(2|F|^{\frac{1}{2}}y - i\frac{\theta_2}{2}\right)\right]} \right]^N dy. \tag{27}$$

where we have written the whole integral as an exponential. We can evaluate the integral in the large N limit using the *saddle-point technique*.

$$\lim_{N\to\infty} \frac{1}{N} \ln Z(J,B) = \ln 2 +$$
$$+ \lim_{N\to\infty} \frac{1}{N} \ln \int_{-\infty}^{\infty} \left[e^{-y^2 + \frac{1}{2}\ln\left[\cosh^2\left(2|F|^{\frac{1}{2}}y\right) - \sin^2\frac{\theta}{2}\right]} \right]^N dy. \tag{28}$$

The maximum of

$$g(y) = -y^2 + \frac{1}{2}\ln\left[\cosh^2\left(2|F|^{\frac{1}{2}}y\right) - \sin^2\frac{\theta}{2}\right] \tag{29}$$

gives us the saddle-point equations

$$-y_0 + \frac{|F|^{\frac{1}{2}}}{2} \frac{\sinh\left(4|F|^{\frac{1}{2}}y_0\right)}{\cosh^2\left(2|F|^{\frac{1}{2}}y_0\right) - \sin^2\frac{\theta}{2}} = 0, \tag{30}$$

$$-1 + 2|F| \frac{\cos^2\frac{\theta}{2}\cosh\left(4|F|^{\frac{1}{2}}y_0\right) - \sinh^2\left(2|F|^{\frac{1}{2}}y_0\right)}{\cosh^2\left(2|F|^{\frac{1}{2}}y_0\right) - \sin^2\frac{\theta}{2}} < 0. \tag{31}$$

Thus, the free energy is

$$f(F,h) = \ln 2 + g(y_0) \tag{32}$$

where y_0 verifies (30), (31).

We can also evaluate the magnetizations:

$$m_1 = \frac{1}{2}\frac{\cosh\left(2|F|^{\frac{1}{2}}y_0\right)\sinh\left(2|F|^{\frac{1}{2}}y_0\right) + i\sin\frac{\theta}{2}\cos\frac{\theta}{2}}{\cosh^2\left(2|F|^{\frac{1}{2}}y_0\right) - \sin^2\frac{\theta}{2}}, \tag{33}$$

$$m_2 = -\frac{1}{2}\frac{\cosh\left(2|F|^{\frac{1}{2}}y_0\right)\sinh\left(2|F|^{\frac{1}{2}}y_0\right) - i\sin\frac{\theta}{2}\cos\frac{\theta}{2}}{\cosh^2\left(2|F|^{\frac{1}{2}}y_0\right) - \sin^2\frac{\theta}{2}}, \tag{34}$$

$$m = \frac{i\sin\frac{\theta}{2}\cos\frac{\theta}{2}}{\cosh^2\left(2|F|^{\frac{1}{2}}y_0\right) - \sin^2\frac{\theta}{2}}, \tag{35}$$

$$m_S = \frac{\cosh\left(2|F|^{\frac{1}{2}}y_0\right)\sinh\left(2|F|^{\frac{1}{2}}y_0\right)}{\cosh^2\left(2|F|^{\frac{1}{2}}y_0\right) - \sin^2\frac{\theta}{2}}. \tag{36}$$

Therefore, and using (30),

$$y_0 = |F|^{\frac{1}{2}} \langle m_S \rangle. \tag{37}$$

In order to compute the gap in the susceptibilities at the critical line, we must examine the behaviour of the variable y_0 in the neighbourhood of θ_c. The way to proceed is to expand the hyperbolic functions in (30) as a power series in y_0. For $\theta < \theta_c$ the only solution to the saddle point equation is $y_0 = 0$, so we expand around this point

$$\sinh\left(4\,|F|^{\frac{1}{2}}\,y_0\right) = 4\,|F|^{\frac{1}{2}}\,y_0 + \frac{32}{3}\,|F|^{\frac{3}{2}}\,y_0^3 + O\left(y^5\right), \tag{38}$$

$$\cosh\left(2\,|F|^{\frac{1}{2}}\,y_0\right) = 1 + 2\,|F|\,y_0^2 + O\left(y^4\right), \tag{39}$$

so the saddle-point equation becomes

$$y_0 \sim 2\,|F|\,\frac{y_0 + \frac{8}{3}\,|F|\,y_0^3}{4\,|F|\,y_0^2 + \cos^2\frac{\theta}{2}} \qquad y_0 << 1. \tag{40}$$

Now we expand again the denominator of (40) up to y_0^2,

$$\frac{1}{4\,|F|\,y_0^2 + \cos^2\frac{\theta}{2}} = \frac{1}{\cos^2\frac{\theta}{2}} - \frac{4\,|F|}{\cos^4\frac{\theta}{2}}y_0^2 + O\left(y_0^4\right). \tag{41}$$

Therefore, for $\theta \gtrsim \theta_c$,

$$y_0 \sim \frac{2\,|F|}{\cos^2\frac{\theta}{2}}y_0 + 8\,|F|^2\,\frac{2\cos^2\frac{\theta}{2} - 3}{3\cos^4\frac{\theta}{2}}y_0^3. \tag{42}$$

We already know of the $y_0 = 0$ solution. Solving the quadratic equation that is left,

$$y_0 = \sqrt{\frac{3}{8\,|F|^2}\frac{\left(\cos^2\frac{\theta}{2} - 2\,|F|\right)\cos^2\frac{\theta}{2}}{2\cos^2\frac{\theta}{2} - 3}}. \tag{43}$$

Thus y_0 tends to zero as θ approaches the critical value for a given F. Its derivative with respect to θ, on the other hand,

$$\frac{dy_0}{d\theta} = -\sqrt{\frac{3}{32\,|F|^2}}\frac{\sin\theta\left(\cos^4\frac{\theta}{2} - 3\cos^2\frac{\theta}{2} + 3\,|F|\right)}{\sqrt{\left(2\cos^2\frac{\theta}{2} - 3\right)^3\left[\left(\cos^2\frac{\theta}{2} - 2\,|F|\right)\cos^2\frac{\theta}{2}\right]}}, \tag{44}$$

diverges as

$$\frac{1}{\sqrt{\left(\cos^2\frac{\theta}{2} - 2\,|F|\right)\cos^2\frac{\theta}{2}}},$$

for at the critical line $\cos\frac{\theta_c}{2} = 2F$. The divergence cancels in the product $y_0\frac{dy_0}{d\theta}$. As $y_0 = \sqrt{|F|}m_S$, this also applies to $m_S\frac{dm_S}{d\theta}$.

The solution obtained in (43) can be used to calculate the behaviour of the susceptibilities around the critical point. The 'topological' susceptibility

$$\chi_T = \frac{dm}{di\frac{\theta}{2}} = \frac{dm}{d\theta}\frac{d\theta}{di\frac{\theta}{2}} = \frac{\left(\cos^2\frac{\theta}{2} - 1\right)\cosh\left(2\,|F|\,m_S\right) + 1 - \cos^2\frac{\theta}{2}}{\left(\cosh^2\left(2\,|F|\,m_S\left(\theta\right)\right) - \sin^2\frac{\theta}{2}\right)^2} -$$

$$- \frac{2\,|F|\sin\theta\sinh\left(4\,|F|\,m_S\right)\frac{dm_S}{d\theta}}{\left(\cosh^2\left(2\,|F|\,m_S\right) - \sin^2\frac{\theta}{2}\right)^2}, \tag{45}$$

takes the value

$$\lim_{\theta\to\theta_c^-}\chi_T = \frac{1}{\cos^2\frac{\theta_c}{2}} = \frac{1}{2\,|F|}, \tag{46}$$

as we approach θ_c from below. However, if we come from the antiferromagnetic phase $\theta > \theta_c$, the second term gives a non-zero contribution, for the derivative $\frac{dm_S}{d\theta}$ diverges at the critical line. The divergence is cancelled exactly by the factor $\sinh(4|F|m_S)$, as explained before, and what remains is a finite contribution

$$m_S \frac{dm_S}{d\theta}\bigg|_{\theta=\theta_c} = -\frac{3\sin\theta_c}{16|F|^2(4|F|-3)}$$

$$\frac{2|F|\sin\theta\sinh(4|F|m_S)\frac{dm_S}{d\theta}}{\left(\cosh^2(2|F|m_S)-\sin^2\frac{\theta}{2}\right)^2} \sim -\frac{3\sin^2\theta_c}{32|F|^2(4F-3)}$$

. In the end

$$\lim_{\theta\to\theta_c^+}\chi_T = \frac{1}{2|F|} + \frac{3}{4|F|}\frac{2|F|-1}{4|F|-3}, \tag{47}$$

and the gap is

$$\Delta\chi_T = \lim_{\theta\to\theta_c^+}\chi_T - \lim_{\theta\to\theta_c^-}\chi_T = \frac{3}{4|F|}\frac{2|F|-1}{4|F|-3}. \tag{48}$$

The staggered susceptibility diverges at the critical line. This is quite expected, as for $\theta=0$ the susceptibility diverges at the critical point. In order to obtain χ_S, we need to take derivatives with respect to a staggered field θ_S, and then take the $\theta_S \to 0$ limit. To this purpose, we use the original form of the free energy (A) with a θ_S term

$$f(F,m_S,\theta,\theta_S) = -|F|m_S^2 + \frac{1}{2}\ln\left[\cosh\left(2|F|m_S + \frac{i\theta+i\theta_S}{2}\right)\times\right.$$
$$\left.\cosh\left(2|F|m_S - \frac{i\theta-i\theta_S}{2}\right)\right] \tag{49}$$

Taking derivatives with respect to m_S we should recover the saddle-point equation with the addition of the θ_S source

$$\frac{df}{dm_S} = 0 = -2|F|m_S + |F|\left[\tanh\left(2|F|m_S + \frac{i\theta+i\theta_S}{2}\right)+\right.$$
$$\left.\tanh\left(2|F|m_S - \frac{i\theta-i\theta_S}{2}\right)\right]. \tag{50}$$

From (A) a new equation for the staggered magnetization is obtained

$$m_S = \frac{1}{2}\left[\tanh\left(2|F|m_S + \frac{i\theta+i\theta_S}{2}\right)+\right.$$
$$\left.\tanh\left(2|F|m_S - \frac{i\theta-i\theta_S}{2}\right)\right]. \tag{51}$$

The derivative with respect to θ_S gives us the susceptibility

$$\chi_S = \frac{dm_S}{d\frac{i\theta_S}{2}} = \frac{1+2|F|\chi_S}{2\cosh^2\left(2|F|m_S + \frac{i\theta+i\theta_S}{2}\right)}+$$
$$\frac{1+2|F|\chi_S}{2\cosh^2\left(2|F|m_S - \frac{i\theta-i\theta_S}{2}\right)} = \frac{1+2|F|\chi_S}{2}X, \tag{52}$$

where

$$X = \frac{1}{2\cosh^2\left(2|F|m_S + \frac{i\theta+i\theta_S}{2}\right)} + \frac{1}{2\cosh^2\left(2|F|m_S - \frac{i\theta-i\theta_S}{2}\right)}.$$

Moving all the terms proportional to χ_S to the l.h.s.

$$2\chi_S(1-|F|X) = X, \tag{53}$$

we can find the value of χ_S

$$\chi_S = \frac{X}{2 - 2\,|F|\,X}. \tag{54}$$

The quantity X must be evaluated at the point $\theta = \theta_c$ and $\theta_S = 0$. This is not a difficult task and the final value is

$$X = \frac{1}{|F|}.$$

The staggered susceptibility, on the other hand, diverges at the critical line. Approaching the critical point from the high temperature region (where the only solution to the saddle point equation is $m_S = 0$), we find

$$\chi_S = \frac{1}{2\,|F_c| - 2\,|F|}, \tag{55}$$

the susceptibility diverges at the critical line $F = F_c$ and the critical exponent for this divergence

$$\chi_S \propto |T - T_c|^{-\gamma_S} \tag{56}$$

is $\gamma_S = 1$.

Finally, and to elucidate the behaviour of $m(\theta)$ as $\theta \to \pi$, we need to work out the following limit

$$\lim_{\theta \to \pi} \frac{dm_S}{d\theta} \sin\theta. \tag{57}$$

As $\sin\theta \to 0$ when θ approaches π, only if the derivative $\frac{dm_S}{d\theta}$ diverges at $\theta = \pi$ is the product (57) non-vanishing. The expansion we performed previously is not very useful here, as the point $\theta = \pi$ is far from the critical line (unless we are taking the $F \to 0$ limit as well). The way to solve this problem is to compute implicitly the derivative from the saddle-point equation (17) at $\theta = \pi$

$$\begin{aligned}
\left.\frac{dm_S}{d\theta}\right|_{\theta=\pi} &= \left.\frac{dm_S}{d\theta}\,\frac{2\,|F|\cosh\left(4\,|F|\,m_S\right)}{\cosh^2\left(2\,|F|\,m_S\right) - \sin^2\frac{\theta}{2}}\right|_{\theta=\pi} - \\
&- \sinh\left(4\,|F|\,m_S\right)\left.\frac{\frac{dm_S}{d\theta}\,|F|\sinh\left(4\,|F|\,m_S\right) - \frac{\sin\theta}{4}}{\left(\cosh^2\left(2\,|F|\,m_S\right) - \sin^2\frac{\theta}{2}\right)^2}\right|_{\theta=\pi} = \\
&= \left.\frac{dm_S}{d\theta}\right|_{\theta=\pi} 4\,|F|\ \mathrm{cotanh}\ \left(2\,|F|\,m_S\right)\left[1 -\ \mathrm{cotanh}\ \left(2\,|F|\,m_S\right)\right].
\end{aligned} \tag{58}$$

Moving all the terms to the l.h.s. of the equation we find that either

$$1 - 4\,|F|\ \mathrm{cotanh}\ \left(2\,|F|\,m_S\right)\left[1 -\ \mathrm{cotanh}\ \left(2\,|F|\,m_S\right)\right] = 0, \tag{59}$$

or

$$\left.\frac{dm_S}{d\theta}\right|_{\theta=\pi} = 0. \tag{60}$$

The first case is impossible, for the solution to the saddle-point equation at $\theta = \pi$ imposes

$$m_S(\pi) =\ \mathrm{cotanh}\ \left(2\,|F|\,m_S\right), \tag{61}$$

which is non-zero and verifies

$$|m_S| \geq 1,$$

so the l.h.s. never vanishes, for the second summand is always positive. Therefore, (60) applies and the derivative vanishes at $\theta = \pi$.

References

[1] V. Azcoiti, G. Di Carlo, A. Galante and V. Laliena, *Phys. Lett. B* **563**, (2003) 117.

[2] F.D.M. Haldane, *Phys. Lett. A* **93**, (1983) 464; *Phys. Rev. Lett.* **50**, (1983) 1153.

[3] J. Plefka and S. Samuel, *Phys. Rev. D* **56**, (1997) 44.

[4] M. Imachi, S. Kanou and H. Yoneyama, *Prog. Theor. Phys.* **102**, (1999) 653.

[5] U. Wolff, *Phys. Rev. Lett.* **62**, (1989) 361.

[6] W. Bietenholz, A. Pochinsky, U.J. Wiese, *Phys. Rev. Lett.* **75**, (1995) 4524.

[7] J. Ambjorn, K.N. Anagnostopoulos, J. Nishimura, J.J.M. Verbaarschot, *JHEP* **0210**, (2002) 062.

[8] L. Del Debbio, H. Panagopoulos and E. Vicari, *JHEP* **0208**, (2002) 044.

[9] M. D'Elia, *Nucl. Phys. Proc. Suppl.* **133**, (2004) 285.

[10] B.B. Beard, M. Pepe, S. Riederer, U.-J. Wiese, *Comput. Phys. Commun.* **175**, (2006) 629.

[11] M. Imachi, Y. Shinno, H. Yoneyama, *Prog. Theor. Phys.* **115**, (2006) 931.

[12] B. Alles, A. Papa, *Phys. Rev. D* **77**, (2008) 056008.

[13] V. Azcoiti, G. Di Carlo, A. Galante and V. Laliena, *Phys. Rev. Lett.* **89**, (2002) 141601.

[14] V. Azcoiti, G. Di Carlo, A. Galante and V. Laliena, *Phys. Rev. D* **69**, (2004) 056006.

[15] S. G. Brush, *Rev. Mod. Phys.* **39**, (1997) 883.

[16] M. Niss, *Arch. Hist. Exact. Sci.* **59**, (2005) 267.

[17] W. Lenz, *Phys. Zeitschr.* **21**, (1920) 613.

[18] P. Curie, *Ann. Chim. Phys.* **5**, (1895) 289; *Oeuvres*, p. 232.

[19] P. Weiss, *J. de Physique* **6**, (1907) 667.

[20] P. Langevin, *J. de Physique* **4**, (1905) 678; *Annales de Chimie et Physique* **5**, (1905) 70.

[21] E. Ising, *Zeitschr. f. Physik* **31**, (1925) 253.

[22] R. Peierls, *Proc. Cambridge Phil. Soc.* **32**, (1936) 477.

[23] H. A. Kramers and G. H. Wannier, *Phys. Rev.* **60**, (1941) 252.

[24] E. Montroll, *J. Chem. Phys.* **9**, (1941) 706; *J. Chem. Phys.* **10**, (1942) 61;

[25] L. Onsager, *Phys. Rev.* **65**, (1944) 117.

[26] John B. Kogut, *Rev. Mod. Phys.* **51**, (1979) 659.

[27] V. Azcoiti, V. Laliena, and A. Galante, Proceedings of the *International Workshop on Non-Perturbative Methods and Lattice QCD*, Guangzhou, China, (2000) 161 [`hep-lat/0007045`].

[28] V. Azcoiti, G. Di Carlo and A. Galante, *Phys. Rev. Lett.* **98**, (2007) 257203 [`arXiv:0710.1507 [hep-lat]`].

[29] T. D. Lee and C. N. Yang, *Phys. Rev.* **87**, (1952) 410.

[30] V. Matveev and R. Shrock, *J. Phys. A* **28**, (1995) 4859.

[31] R. Agra, F. van Wijland and E. Trizac, *Eur. J. Phys.* **27**, (2006) 407.

[32] For a recent review see E. Vicari and H. Panagopoulos, *Phys. Rep.* **470**, (2009) 93.